

Seismic Background Noise Levels in Italian Strong Motion Network

Simone Francesco Fornasari¹, Deniz Ertuncay¹, and Giovanni Costa¹

¹SeisRaM Working Group, Department of Mathematics and Geosciences, University of Trieste, Via Eduardo Weiss 4, 34128 Trieste, Italy

Correspondence: Simone Francesco Fornasari (simonefrancesco.fornasari@phd.units.it)

Abstract. Italian strong motion network monitors the seismic activity in the region with more than 585 stations with continuous data acquisition. In this study, we determine the background seismic noise characteristics of the network by using the data collected in 2022. We analyze the spatial and temporal characteristics of the background noise. It is found that most of the stations suffer from anthropogenic noises since the strong motion network is designed to capture the peak ground motions in populated areas. Hence human activities enrich the low periods of noise. Therefore, land usage of the area where the stations are located affects the background noise levels. Stations can be noisier during the day, up to 12 decibels, and during the weekday, up to 5 decibels, in short periods. In long periods (≥ 5 s), accelerometric stations converge to similar noise levels and there are no significant daily or weekly changes. It is found that more than half of the stations exceed the background noise model designed for strong motion stations in Switzerland by Cauzzi and Clinton (2013) in at least one of the calculated periods. We also develop an accelerometric seismic background noise model for periods between 0.0124 s to 100 s for Italy by using the power spectral densities of the network. The model is in agreement with the background noise model developed by D’Alessandro et al. (2021) using broadband data for Italy in short periods but in long periods there is no correlation among studies.

1 Introduction

Seismic stations record the vibration of the ground that is given by the superposition of multiple sources. The definition of seismic noise varies based on the target of each specific study. Since most of the seismic networks are established to detect seismic events (i.e., earthquakes, volcanic activities, quarry blasts, and nuclear explosions) all other vibrations are referred to as (ambient) noise. On the other hand, ambient noise itself has been the object of specific studies (e.g., for the characterization of layers of the earth (Shapiro et al., 2005), Moon (Larose et al., 2005), and Mars (Schimmel et al., 2021)). Noises can also be sub-categorized based on their source such as; i) recorders (Ringler and Hutt, 2010), ii) temperature changes (Stutzmann et al., 2000; Doody et al., 2018), iii) ocean and sea waves (Webb, 1998; McNamara and Buland, 2004; Bonnefoy-Claudet et al., 2006; Cauzzi and Clinton, 2013; D’Alessandro et al., 2021; Anthony et al., 2022), iv) gravity-gradient noise (Harms et al., 2009), v) wind (Mucciarelli et al., 2005; Bonnefoy-Claudet et al., 2006; D’Alessandro et al., 2021; Anthony et al., 2022), vi) human activities (McNamara and Buland, 2004; Bonnefoy-Claudet et al., 2006; Cauzzi and Clinton, 2013; Vassallo et al., 2019; D’Alessandro et al., 2021; Anthony et al., 2022) (Figure 1).

The level of noise affects the quality of the recorded waveforms, hence the ability to detect seismic events. To be able to monitor the seismic sources, seismic networks require knowledge about the noise content of the networks. To characterize the noise at a given station, the frequency content of the noise is calculated via power spectrum density (PSD). The above-mentioned noise sources can be seen in different frequency bands of the PSD (Figure 1). Various models have been created to interpret the noise levels. The model of Peterson (1993) is widely used to define the lower (New Low Noise Model, NLNM) and upper (New High Noise Model, NHHM) bounds of the recorded noise as a baseline, developed using a worldwide catalogue from a wide variety of seismic stations. Cauzzi and Clinton (2013) developed the accelerometer low-noise (ALNM) and high-noise (AHNM) models using accelerometric data from the Swiss Seismological Service (Clinton et al., 2011) and very broad-band along with accelerometric data from Southern California Seismic Network (California Institute of Technology and United States Geological Survey Pasadena, 1926). The AHNM is computed as the lower boundary of 5-percentile PSD amplitudes observed on rock sites in which urban noise, microseismic activities, and data logger systems dominate the short periods, mid-range periods, and long periods, respectively. The ALNM is computed as a particular combination of accelerometric sensors with a given gain and response with dataloggers. This model is widely used as the baseline model for strong motion sensors (Ringler et al., 2015, 2020).

The National Accelerometric Network (RAN), owned and managed by the Italian Civil Protection Department (DPC) (Presidency of Council of Ministers - Civil Protection Department, 1972; Gorini et al., 2010; Zambonelli et al., 2011; Costa et al., 2022), is established to monitor strong motions at a national level. The integrated RAN is the combination of RAN with the following networks; i) the Friuli Venezia Giulia and Veneto Accelerometric Network (RAF, Rete Accelerometrica Friuli Venezia Giulia in Italian, University of Trieste 1993; Costa et al. 2010) in North-East Italy, owned and managed by the University of Trieste (UniTS) ii) Irpinia Seismic Network (ISNet, Weber et al. 2007) in the South of Italy, owned and managed by Analysis and Monitoring of Environmental Risk Society (AMRA). Thereinafter, RAN will refer to the integrated RAN. Being the RAN main goal to provide information valuable for Civil Protection duties, the selection criteria of the “optimal” location to install seismic stations weighs multiple parameters and the quality of the recordings in terms of noise generated by nearby sources could play a secondary role.

In this paper, we focus on the background noise in RAN by analyzing the data recorded by 585 continuous stations during 2022 and developed the Italian accelerometric noise models. We focused our analysis mainly on the short periods (≤ 5 s) since they carry more relevant information related to parameters useful for civil defence purposes (e.g., PGA, PSA0.3, PSA1.0, and PSA3.0). The progressive conversion of data acquisition from triggered to continuous recording starting from the end of 2020 increased the number of stations available to study noise levels on a national scale.

In Section 2, we explain the properties of RAN and the time coverage of the data. In Section 3, the data preprocessing, PSD evaluation workflow, and development of the Italian accelerometric noise models are explained. Background noise levels and the noise models are presented in Section 4 and the possible noise sources, temporal and spatial variations of noise, and comparison between previous background noise models with the developed model are discussed in Section 5.

2 Data

60 In this study, data from the vertical component of 585 stations of the RAN collected in 2022 have been analyzed (Figure 2). RAN stations have generally a standardized installation near urban areas (see Table 1) in free-field conditions, with instruments placed on an isolated pillar anchored on rock or put inside of the sediments. On average, 383 of these stations were operational in continuous recording for more than 90 % of the year. We set a threshold of 50 % of completeness of PSD time series for data selection to calculate the background noise model for the RAN which makes 494 out of 585 stations (84.6 % of stations) 65 eligible for the further steps: the remaining stations operated either in triggered mode throughout the year or converted into continuous data recording later in the year.

Seismic instruments of the network consist mostly of Kinematics and Syscom sensors (Table 2) with 24 bit acquisition. Data transfer from the station to the data centre in Rome, Italy is carried out mainly by an Access Point Name (APN) dedicated to RAN and a copy of the data is sent to Trieste (Italy) via a Virtual Private Network (VPN).

70 The evolution of the RAN is not only about the combination of several networks but also the installation of new stations across the Italian territory over time. Moreover, the data acquisition systems of the network have changed over time. After 2020, a large number of triggered stations have been replaced with continuous data acquisition. The purpose of the RAN is to determine the ground motion parameters recorded in the areas where there is considerable human activity. RAN provides valuable information to the Italian civil defence (DPC) to help in decision-making after seismic events. Because of that, factors 75 that affect the quality of the seismic waveforms recorded (i.e., background noise levels and soil conditions) may not be the main priority for DPC in deciding where a new station is going to be deployed. Most of the RAN stations (Table 3) sit on top of a *B* and *C* class soil (Aucun et al., 2012) and many of the stations are located in the settlements (Table 1).

3 Method

The method introduced by McNamara and Buland (2004) represents the de facto standard for the evaluation of PSDs. This 80 method was originally developed as a tool for monitoring the status of seismic stations: as such, the original parameters used for the computation of the PSDs and the use of smoothing and averaging provide a way to reduce the storage and computation costs involved, but can be limiting when the method is extended to scientific uses, as shown by Anthony et al. (2020).

The method implemented to compute the PSDs partially mirrors the one by Anthony et al. (2022), which in turn is an adaptation of McNamara and Buland (2004). Considering only the vertical components at the stations, each daily recording in 85 acceleration is divided into 90 min windows with 50 % overlap, each one subsequently divided into 15 min subwindows with 75 % overlap: as pointed out by Anthony et al. (2020), the window length becomes less relevant for higher frequencies and noisier stations, which are the conditions of the present study. Data completeness above 90 % is required for each 90 min window. Transient signals, consisting also of earthquakes, are not removed from the seismic traces since they are low-probability occurrences with respect to ambient seismic noise (McNamara and Buland, 2004): Anthony et al. (2020) showed that while 90 the presence of earthquakes in the recordings can skew the median ambient-noise estimates for longer periods (10 s-50 s), no significant effects have been observed for short periods. During preprocessing, data are linearly detrended, the gaps are linearly

interpolated, and a Hann window is applied to limit spectral leakage (Peterson, 1993; Anthony et al., 2022). For each 15 min subwindow the PSD is computed using Welch's method (Welch, 1967), the results for all the subwindows within each 90 min window are averaged, and the instrument response is then removed from the PSD. No binning and smoothing are performed during the PSDs computation. Similar to Anthony et al. (2022), we performed a one-third octave average over the PSDs: the averaging bandwidth can be assumed as a reasonable trade-off between the obtained spectral resolution and the accuracy in the broadband noise sources characterization in each band. The parameters used for the evaluation of the PSDs in our study, along with the ones used in McNamara and Buland (2004), D'Alessandro et al. (2021), and Anthony et al. (2022) are reported in Table 4.

To study specific patterns in the noise levels over time, the PSDs are studied by grouping them over different time ranges. To study the effects of anthropogenic noise it is a common practice to consider the variations between day (08:00 - 18:00) and night (20:00 - 07:00) and between weekday (Monday - Friday) and weekend (Saturday - Sunday). Similarly, the variations between summer and winter are analysed to check seasonal variations of the noise levels. Stations with more than 50 % of data for both summer and winter time periods are selected to analyze seasonal effects. The statistics related to these variations are computed over the daily difference of the medians of each group.

4 Results

The method explained in the previous section is applied to all the stations in RAN to create the Italian accelerometric high (IAHNM) and low (IALNM) noise models (Figure 3). Amplitudes for each period are given in Table S1 for IAHNM and IALNM. In low periods (≤ 0.1 s) median of the RAN is closer to the higher end of the noise model developed by Cauzzi and Clinton (2013). Between (≤ 0.02 s) to (≤ 0.1 s) IAHNM exceeds the AHNM and between the periods IAHNM and IALNM cover a large range between -124 dB to -84 dB. IAHNM is in a downtrend between (≤ 0.08 s) to around 1 s and it goes upward in the longer periods whereas IALNM is in general upward trend. Around 1 s median of the RAN exceeds the AHNM and IAHNM is greater than AHNM between 0.5 s to 3.5 s. The upwards trend of background noise can be seen in both models but in our study such trend is smoother than the model of Cauzzi and Clinton (2013).

The lower limit of the noise model, IALNM, is, on average, 15 dB higher than the ALNM of Cauzzi and Clinton (2013) which is defined as the theoretical lower boundary of the station noise. Figure 4 shows that only a small amount of stations goes below the IALNM and even these stations cannot reach the ALNM model. PSD values are concentrated in a narrow band in long periods (≥ 5 s) and in short periods they cover a wide range of values. Station locations play an important role in noise characterization (Figure 5). Most of the stations that are located in settlements have high levels of noise, hence increasing the upper boundary of the IAHNM. Even though land usage influences short periods, its effect on long periods shows no clear pattern.

Being RAN a strong motion network, we are mainly interested in periods less than 5 s: afterwards we focus on the specific period bands centred around 0.1 s, 0.25 s, 0.5 s, 1 s, 2 s, and 5 s. We would like to provide an overview of the behaviour of the noise at different timescales for different periods, as described in detail afterwards (see Figure 1). The overall background

125 noise levels for all stations in RAN are presented in Figure 6. The period-wise median of the PSDs for each station is computed and interpreted as the representative noise level. Anthropogenic sources can have a major role in the noise content of short periods (Figure 1) which provide essential information for seismic parameters estimation, seismic engineering and building monitoring. Noise level statistics of RAN stations for each period of interest are reported in Table S2 with the related noise level and the station placement.

130 RAN has relatively high noise levels in short periods with numerous stations exceeding the levels defined by Cauzzi and Clinton (2013). The median noise at each station, presented in Figure 6, and the AHNM have been compared and the results are reported in Table 5. 1 s is the period for which we have the highest rate of exceedance of the AHNM level with 34.4 % of the stations. The probability density function calculated over the median PSD of all stations can be seen in Figure 3. The median values for 0.1 s, 0.25 s, 0.5 s, 1 s, 2 s, and 5 s are -112.59 dB, -119.09 dB, -120.35 dB, -119.98 dB, -118.07 dB, 135 and -115.98 dB, respectively. The median values are always below the AHNM model for the period range of interest. Between 0.1 s and 2 s, stations located in the Po valley and the area from Ischia Island to Naples have relatively high noise levels. Stations around Naples and Ischia Island have the same trend in higher periods.

Under the common assumption that anthropogenic noise decreases during the night hours and the weekend, we characterised the contribution of human activities to ambient noise levels. In 2022, at 493 stations there is a reduction in noise levels at 140 nighttime with respect to the average noise during daytime (Figure 7). Daytime-nighttime noise level change reduces with increasing periods at 0.1 s, 0.25 s, 0.5 s, 1 s, and 2 s with median values of 6.00 dB, 1.45 dB, 0.30 dB, 0.11 dB, and 0.14 dB, respectively. Among these periods 491, 489, 480, 447, and 439, and 475 stations are noisier during the daytime.

We also studied the changes in the noise levels between weekdays and weekends and the general trend of noisier weekdays are observed (Figure 8), consistently with the assumption of a reduction in human activities during the weekends. Median 145 changes between weekdays and weekends are smaller with respect to the daytime-nighttime changes with the same trend of decreasing differences with increasing periods. Weekday - weekend median differences are 0.88 dB, 0.36 dB, 0.08 dB, -0.01 dB, -0.10 dB, and -0.02 dB for 0.1 s, 0.25 s, 0.5 s, 1 s, 2 s, and 5 s, respectively. The general trend of noisier weekdays can be followed between 0.1 s to 0.5 s with 453, 453, and 414 stations in the periods of interest. In the periods between 1 s to 5 s only 215, 52, and 190 stations are noisier in the weekends.

150 To see the seasonal changes in the long periods which can be affected by the marine and atmospheric sources we analyzed the stations in their median summer and winter (McNamara and Buland, 2004) noise level changes (Figure 9) by defining 21st of June to 21st of September as summer and 21st of December to 21st of March as winter. Surprisingly in long periods summer time is noisier than the winter time in 5 s, 8 s, 16 s, and 30 s. These periods are chosen to visualize the effect of the long period background noise at network level. Previous studies (eg. McNamara and Buland (2004); Anthony et al. (2022)) 155 have found the opposite behaviour in the stations. In total the median difference between summer and winter are 0.19 dB, 0.97 dB, 1 dB, and 0.75 dB, for 5 s, 8 s, 16 s, and 30 s, respectively. The purpose of the accelerometric network is to detect the peak ground parameters in destructive earthquakes. Parameters such as peak ground acceleration (PGA) and peak spectral acceleration (PSA) in short periods provide meaningful information about the possible damage in a site of interest and these

parameters are, in general, arrive to the station in the high frequencies of its spectrum. Hence, high background noise levels in
160 long periods do not affect the capabilities of the RAN.

5 Discussion

Table 1 shows the distribution of the stations according to the classification proposed by Istituto Superiore per la Protezione
e la Ricerca Ambientale (2022). Even though most of the stations are located in urban areas and potentially subjected to high
levels of anthropogenic noise, this classification is too reductive (e.g., not considering the population density and the presence
165 or making a distinction between residential and industrial areas) to be associated with specific noise levels.

The interpretation of the background noise in the RAN can be done in three different ranges that are low periods (<1 s),
medium range periods (between 1 s and 5 s), and long periods, (>5 s). As mentioned before, in the low periods, human activities
are the main source of background noise. 291 of 493 stations have noise levels exceeding the AHNM developed by Cauzzi
and Clinton 2013, as reported in Table 5 considering the results for different periods. In Table 5 the highest percentage of
170 stations exceeding the AHNM is at 1 s. This can be due to the specific datalogger systems used by RAN, as discussed by
Cauzzi and Clinton (2013), that shift the background noise levels up and cause network-wide high noise level (Figure 6) at
this specific period. Furthermore, both the geological and anthropogenic settings of Switzerland present some differences from
the Italian ones. Different geodynamic forces act on Italy which creates diverse geological structures in the territory whereas
in Switzerland the geology is more homogeneous. The cultural noise is also different between the two countries: the stations
175 used in Cauzzi and Clinton (2013) are, with the exception of the ones in Basel, mainly located in the countryside or in small
settlements, with respect to the RAN stations.

The potential relation between the geological settings and the background noise characteristics in low periods is also inves-
tigated. Stations located in Po valley, having large alluvial deposits, have relatively high noise levels (Figure S2, Cocco et al.
2001). However, there are other noisy stations that are located in completely different geological settings such as the ones in
180 Naples (local geology is dominated by intrusive rocks). Hence, high background noise cannot be directly linked to the local
geology but the anthropogenic activities. Marzorati and Bindi (2006) analyzed the station in and around the Po valley in terms
of background noise by linking the high noise levels to industrial activities and comparing the considerable noise level changes
with respect to the stations in the North of Po Valley. A similar trend can be seen in our results as well (Figure S2). Stations
located in the North-East of Po Valley (where local geology is dominated by carbonate rocks) are some of the quietest stations
185 in the RAN network due to the lack of human activity.

The effect of human activity on noise levels can be seen by comparing daytime noise to nighttime noise, for which human
activity is reduced. As seen in Figure 7, the majority of the stations are noisier during the day for periods less than 1 s. The noise
difference between day and night decreases with increasing periods, but the nationwide trend of days being noisier is valid for
0.1 s, 0.25 s, and 0.5 s. The same pattern can be seen in broadband stations located in Italy (D'Alessandro et al., 2021). During
190 the daytime anthropogenic sources (e.g. factories, offices, public buildings, vehicles) may enrich the low period portion of the
background noise. During nighttime, most of these activities are either reduced or completely stopped. In North-East Italy, there

are several stations with relatively low daytime-nighttime difference. These stations are located far away from all settlements and located on mountainous parts of Italy. A similar trend can be seen in central Italy in 0.25 s and 0.5 s. Le Gonidec et al. (2021) showed that vehicle noise enrich the periods between 0.067 s and 0.1 s in seismic signals. In 0.1 s nationwide daytime - nighttime difference can be linked to vehicles whereas in periods 0.25 s and 0.5 s other anthropogenic noises (eg. movement of individuals) can be active. In both North-East and central Italy, these noises can be minimal. Hence in daytime - nighttime power change there is no significant difference.

In the weekday - weekend variations, the same pattern can be followed in short periods. Figure 8 shows that weekdays were noisier with respect to weekends in almost all stations. The noise level changes are consistent with the changes in weekly human activities. Most of the banks, public buildings, and offices are not working on weekends and on Sundays commercial activities are reduced which may limit human activities. Hence, in short periods, the background noise of weekdays is dominated by labour-related activities. As in daytime - nighttime differences, in both North-East and central Italy, there are minimal power change differences and the same interpretation can be done for the weekday - weekend differences.

In the medium range periods, there are multiple noise sources that have been identified by previous studies (Figure 1). Cauzzi and Clinton (2013) stretches the cultural noise up to 3 s whereas D'Alessandro et al. (2021) indicates that wind and swell related noises are dominant between 1 s to 10 s. Consequently, variations in the noise sources in 2 s and 5 s can be found by analyzing the daily, weekly and seasonal changes.

Day and night differences in medium range periods follow the trend that is seen in shorter periods except in 1 s. In 1 s the day and night differences are nulled at most stations with the notable exception of the stations located in the Po valley, on Ischia island, and in Naples which remain noisier during the day. The majority of the stations exceed the AHNM threshold in 1 s, and the noise levels do not change during the night, which means that the anthropogenic effects are not the dominant source. Even though in 2 s and 5 s there is a general trend of having higher noise levels during the daytime, the power change is very small (0.11 dB and 0.22 dB, respectively). Moreover, the effects of sea, swell, and/or wind at our stations have not been identified and thus, do not have a significant role on the noise levels: analyzing the trend of median and variability of noise levels at the stations as a function of the distance to the coastline (Figure S3), no evident pattern emerges, as also shown in Figure 6. Almost starting from 1 s background noise levels do not vary too much over the network (Figure 4) and the effect of sea, swell and/or wind effect should not significantly alter by these forces.

Considering weekly variations, stations become noisier on weekends ≥ 1 s with decreasing power change. In the Po valley, the general trend of a high noise level diminishes starting from 2 s in average and in the same periods, unlike the day and night difference, weekends follow the same trend. In 1 s central Italy has almost the same noise levels between weekdays and weekends and in both 1 s and 2 s several stations in Central Italy and Sicily coastlines become noisier during the weekend. Previous studies suggest the effects of anthropogenic sources, wind and sea-related activities to be dominant in those periods. As seen in lower periods, human activity increases the weekday noise levels which makes it irrelevant from the observation. Sea and wind might be the source of the observation if they could be in Figure 6 since neither wind nor sea-related noises should be changed between weekdays and weekends. Hence, we do not have a reasonable explanation about the phenomena.

To show the significant effects that the nearby surrounding of a station can have on its noise level we considered two RAF stations, CARC (latitude: 45.652, longitude: 13.770) and DST2 (latitude: 45.658, longitude: 13.801), located in Trieste (in North-East Italy). Despite their proximity (<3 km), they have different noise characteristics. The selection of these two particular stations is further supported by the extensive knowledge of their spatial and administrative information. DST2 station
230 sits on deep Flysh deposits (Figure 10). CARC station is located on the ground floor of the Palazzo Carciotti which is located in the city centre of Trieste and was built in the early 19th century. It crosses with one of the main major roads in the city centre and the building is surrounded by multistory residential buildings. Historically, this area was a salina and the area is filled with a 27 m depth material layer (Fitzko et al., 2007) to cover up the salina to expand the city in the 18th century (Figure S4).

To see the hourly changes in noise levels, 90 min PSDs are plotted, separately (Figure 11). In the lower periods (<1 s) where
235 anthropogenic noises prevail, CARC station is noisier almost in all time ranges. In very short periods (≤ 0.025 s) they converge but in such low periods electromagnetic noises can be the dominant noise source, hence it is expected to have a converged background noise. In the daytime noise levels of CARC station converge to the AHNM between 0.2 s and 1 s. For periods above 0.5 s, day and night differences are similar which may suggest that anthropogenic sources do not have a major role. On the other hand, in shorter periods there are clear day-night patterns at both stations. DST2 station is located in the basement
240 of a small two-story university building (accommodating just a library, a few offices, and a study room) where human activity is rather limited both inside and outside. Moreover, the building is not located near any major road. Different environmental factors may play a role with changing period of the background noise. Both of the stations are located inside buildings, hence wind effect should be minimal. For periods longer than 10 s, both stations have similar background noise levels and the same trend with increasing periods.

245 As shown in Table 5, 308 of all stations exceed the AHNM for at least one period. However, by comparing with the P-wave corner frequencies by Brune (1970), even the 10 noisiest stations theoretically detect the P wave arrival of magnitude 2.7 event starting from 1 km epicentral distance (Figure S5). Since the purpose of RAN is to record peak amplitudes, those stations are useful even for earthquakes with smaller magnitudes and longer epicentral distances.

Measuring the background noise levels of the RAN allows us to understand the earthquake detection capability. As pre-
250 sented in Figure 4 detection of $M \approx 3$ earthquakes is possible by near-fault stations in raw signals with the stations near the IAHNM. In median noise level it is possible to detect $M \approx 2$ in near fault. DPC publish $M \geq 2.5$ earthquakes in quasi real time (<https://ran.protezionecivile.it/EN/>, last access: 02/08/2023). Data filtering algorithm of Gallo et al. (2014) allows us to reduce the background noise to detect ground motion parameters up to 100 km away from the epicenter for $M = 2.5$ earthquakes (Figure S6). Even though earthquakes with small magnitudes are located by the network, they are not published to the public
255 (Costa et al., 2022).

In Figure 6, there are some areas that follow the pattern found by D'Alessandro et al. (2021), such as in Naples, noise levels are higher than in the stations that are East of Naples inland. In 1 s only the stations in Naples are in agreement with D'Alessandro et al. (2021) and in our study noise levels are much higher in other parts of Italy. The same trend can be seen in longer periods (>5 s) in which wind and swell are the dominant noise sources. There are numerous stations located in the
260 Po valley with high noise levels even though they are far away from the sea, and several stations located in the Alps in North

West Italy. In 0.1 s, we have noisy stations in Po valley, Puglia, and the eastern part of Sicily, where our stations are noisier than the ones analyzed in D'Alessandro et al. (2021). However, in short periods our results are in agreement with the study of D'Alessandro et al. (2021) in other parts of Italy. We can conclude that human-made activities dominate the low periods of the noise content and high noise levels can be linked to the activities that are occurring in the area where anthropogenic sources are present. Reduction in human activity can be seen in Figure 7 in which almost all stations have lower noise levels at night with respect to their daytime counterparts.

The model by D'Alessandro et al. (2021) has a notable relevance with our study since, first, it covers the same area of interest and, second, spatial variability of their model has been developed by means of the inverse distance weighted method (Lu and Wong, 2008). H_{INM} of the D'Alessandro et al. (2021) is almost identical with the IAHNM between 0.05 s and 0.3 s which are higher than the AHNM and NHNM of Cauzzi and Clinton (2013); Peterson (1993). The agreement between IAHNM in low periods indicates that both broadband and strong motion networks in Italy get affected by the anthropogenic noises in the same order of magnitude and in periods between 0.05 s and 0.1 s anthropogenic noises have larger effects on the seismic networks with respect to Swiss and the US seismic networks. Around 1 s the most significant divergence among higher limit of the models is observed. AHNM and NHNM are close to the median of our network and the IAHNM is about 10 dB higher than them. Interestingly, H_{INM} has even higher noise levels with respect to our model. Between 5 s and 10 s other models converge whereas our model has a completely different trend. As we discussed before our model is not susceptible to any long-period trends. AHNM and IAHNM have similar trends for periods above 10 s as AHNM developed by using strong motion stations.

The second important outcome of the D'Alessandro et al. (2021) is to model the spatial variance of the noise of the Italian broadband network for 4 different band period bands. This allows us to calculate the predicted noise levels for most of our stations. To compare our noise levels with the predictions of D'Alessandro et al. (2021) we calculate the median of periods that reside in the limits of the bands. The difference between the noise levels in RAN stations and the model developed by D'Alessandro et al. (2021) can be seen in Figure 12. In Band IV ($0.033 \text{ s} \geq T > 0.1 \text{ s}$) of D'Alessandro et al. (2021) anthropogenic sources are the dominant source type and the major cities of Italy (e.g. Milan, Rome, and Naples) have higher noise levels. In this band difference between the background noise of RAN and the model prediction has greater values in the regions where the model prediction is relatively low such as North-East Italy and several parts of South Italy. There are numerous stations with almost no difference between the prediction and observation but there is no overall trend in any geographical location. Since sources of the low period noises are very local, the difference is mostly dominated by local effects. Hence, there are numerous stations with almost zero dB difference located near to stations with larger differences in Central Italy. In Band III both natural and anthropogenic sources are in action and the difference between the noise levels in major cities and relatively rural areas of Italy is can be seen easily in the model of D'Alessandro et al. (2021).

6 Conclusions

The recent modernization of RAN stations allowed us to study their noise levels on a nationwide scale. The analysis is performed by computing PSDs over 90 min windows of signals using continuous recordings acquired in 2022. The results of this

study improve the overall seismic background noise information of Italy, complementing the previous work by D'Alessandro et al. (2021) for the Italian broadband network. It is found that a significant number of stations (up to 51.3% of all stations) have higher noise levels than the AHNM that is defined for accelerometers in Switzerland and California by Cauzzi and Clinton (2013).

As presented in Section 4, RAN has several very noisy stations located within cities. We must stress that the fundamental duty of RAN is to provide ground motions of the locations where civil defence may need to provide assistance in post-disaster (e.g., strong earthquake) situations. Even though some of these stations are noisy (Table 5), they are well capable of providing the true nature of the ground motion if there is a strong earthquake nearby, hence they are able to serve their purpose (Costa et al., 2022). Depending on the nature of the future station installations and studies, noise levels of RAN (Figure 6) may give an insight into the capabilities of the stations.

The daily variations of the noise levels of the station, obtained comparing the daytime (08:00 - 18:00) and nighttime (20:00 - 07:00) results, show that in short periods where human - made activities dominate the seismic records daytime is noisier than nighttime. The difference is relatively low in the stations located on the mountainous parts of North-East Italy.

In the longer periods (≥ 1 s), unlike various previous studies, our analysis has not found any evidence of the swell and sea effect on noise levels (between 1 s and 40 s) with no clear pattern arising considering stations at different distance to the coastline (Figure 6). In periods between 2 s to 5 s winter is noisier as expected from previous studies (D'Alessandro et al., 2021) but in longer periods it is reversed and the median noise differences between winter and summer are generally constant network-wise with values increasing with periods. These results are consistent with the instrumental noise being the main noise source at long periods, as indicated by Cauzzi and Clinton (2013).

Code and data availability. The analysis has been performed using the data and metadata from the Italian Strong Motion Network (RAN, Gorini et al. 2010; Costa et al. 2022). Data and materials along with the developed models can be found in a dedicated GitHub repository.

<https://doi.org/10.5194/nhess-0-1-2023-supplement>

Author contributions. Conceptualisation, all authors.; methodology, S.F.F.; software, S.F.F.; data curation, all authors; writing—original draft preparation, D.E. and S.F.F.; writing—review and editing, all authors; visualisation, S.F.F. and D.E.; supervision, G.C.; project administration, G.C.; funding acquisition, G.C. All authors have read and agreed to the published version of the manuscript.

Competing interests. The contact author has declared that none of the authors has any competing interests.

Acknowledgements. This study received financial support from the Italian Civil Protection - Presidency of the Council of Ministers.

References

- Anthony, R. E., Ringler, A. T., Wilson, D. C., Bahavar, M., and Koper, K. D.: How processing methodologies can distort and bias power spectral density estimates of seismic background noise, *Seismological Research Letters*, 91, 1694–1706, 2020.
- Anthony, R. E., Ringler, A. T., and Wilson, D. C.: Seismic background noise levels across the Continental United States from USArray
325 transportable array: The influence of geology and geography, *Bulletin of the Seismological Society of America*, 112, 646–668, 2022.
- Aucun, B., Fajfar, P., Franchin, P., Carvalho, E., Kreslin, M., Pecker, A., Tsonis, G., Pinto, P., Degee, H., Plumier, A., Fardis, M., Athanasopoulou, A., Bisch, P., and Somja, H.: Eurocode 8 : seismic design of buildings - Worked examples, Publications Office, <https://doi.org/doi/10.2788/91658>, 2012.
- Bonnefoy-Claudet, S., Cornou, C., Bard, P.-Y., Cotton, F., Moczo, P., Kristek, J., and Fäh, D.: H/V ratio: A tool for site effects evaluation.
330 Results from 1-D noise simulations, *Geophysical Journal International*, 167, 827–837, 2006.
- Brune, J. N.: Tectonic stress and the spectra of seismic shear waves from earthquakes, *Journal of Geophysical Research (1896-1977)*, 75, 4997–5009, <https://doi.org/https://doi.org/10.1029/JB075i026p04997>, 1970.
- California Institute of Technology and United States Geological Survey Pasadena: Southern California Seismic Network, <https://doi.org/10.7914/SN/CI>, 1926.
- 335 Cauzzi, C. and Clinton, J.: A high-and low-noise model for high-quality strong-motion accelerometer stations, *Earthquake Spectra*, 29, 85–102, 2013.
- Clinton, J., Cauzzi, C., Fäh, D., Michel, C., Zweifel, P., Olivieri, M., Cua, G., Haslinger, F., and Giardini, D.: The current state of strong motion monitoring in Switzerland, in: *Earthquake Data in Engineering Seismology*, pp. 219–233, Springer, 2011.
- Cocco, M., Ardizzoni, F., Azzara, R. M., Dall’Olio, L., Delladio, A., Di Bona, M., Malagnini, L., Margheriti, L., and Nardi, A.: Broadband
340 waveforms and site effects at a borehole seismometer in the Po alluvial basin (Italy), 2001.
- Costa, G., Moratto, L., and Suhadolc, P.: The Friuli Venezia Giulia Accelerometric Network: RAF, *Bulletin of Earthquake Engineering*, 8, 1141–1157, <https://doi.org/https://doi.org/10.1007/s10518-009-9157-y>, 2010.
- Costa, G., Brondi, P., Cataldi, L., Cirilli, S., Ertuncay, D., Falconer, P., Filippi, L., Fornasari, S. F., Pazzi, V., and Turpaud, P.: Near-Real-Time Strong Motion Acquisition at National Scale and Automatic Analysis, *Sensors*, 22, 5699, 2022.
- 345 Cucchi, F., Piano, C., Fanucci, F., Pugliese, N., Tunis, G., Zini, L., Covelli, S., Fanzutti, G. P., Ponton, M., and Fontana, A.: Carta geologica del Carso Classico, 2013.
- Doody, C., Ringler, A. T., Anthony, R. E., Wilson, D. C., Holland, A. A., Hutt, C. R., and Sandoval, L. D.: Effects of thermal variability on broadband seismometers: Controlled experiments, observations, and implications, *Bulletin of the Seismological Society of America*, 108, 493–502, 2018.
- 350 D’Alessandro, A., Greco, L., Scudero, S., and Lauciani, V.: Spectral characterization and spatiotemporal variability of the background seismic noise in Italy, *Earth and Space Science*, 8, e2020EA001 579, 2021.
- Felicetta, C., Russo, E., D’Amico, M. C., Sgobba, S., Lanzano, G., Mascandola, C., Pacor, F., and Luzi, L.: ITalian ACcelerometric Archive (ITACA), version 4.0, 2023.
- Fitzko, F., Costa, G., Delise, A., and Suhadolc, P.: Site effects analyses in the old city center of Trieste (NE Italy) using accelerometric data,
355 *Journal of Earthquake Engineering*, 11, 33–48, 2007.
- Gallo, A., Costa, G., and Suhadolc, P.: Near real-time automatic moment magnitude estimation, *Bulletin of earthquake engineering*, 12, 185–202, <https://doi.org/https://doi.org/10.1007/s10518-013-9565-x>, 2014.

- Gorini, A., Nicoletti, M., Marsan, P., Bianconi, R., de Nardis, R., Filippi, L., Marcucci, S., Palma, F., and Zambonelli, E.: The Italian strong motion network, *Bulletin of Earthquake Engineering*, 8, 1075–1090, <https://doi.org/https://doi.org/10.1007/s10518-009-9141-6>, 2010.
- 360 Harms, J., Sajeve, A., Trancynger, T., DeSalvo, R., Mandic, V., and Collaboration, L. S.: Seismic studies at the Homestake mine in Lead, South Dakota, LIGO document, pp. T0900 112–v1, 2009.
- Istituto Superiore per la Protezione e la Ricerca Ambientale: Carta Nazionale di Copertura del Suolo, <https://www.isprambiente.gov.it/attivita/suolo-e-territorio/suolo/copertura-del-suolo/carta-nazionale-di-copertura-del-suolo>, 2022.
- Larose, E., Khan, A., Nakamura, Y., and Campillo, M.: Lunar subsurface investigated from correlation of seismic noise, *Geophysical Research Letters*, 32, <https://doi.org/https://doi.org/10.1029/2005GL023518>, 2005.
- 365 Le Gonidec, Y., Kergosien, B., Wassermann, J., Jaeggi, D., and Nussbaum, C.: Underground traffic-induced body waves used to quantify seismic attenuation properties of a bimaterial interface nearby a main fault, *Journal of Geophysical Research: Solid Earth*, 126, e2021JB021 759, <https://doi.org/https://doi.org/10.1029/2021JB021759>, 2021.
- Lu, G. Y. and Wong, D. W.: An adaptive inverse-distance weighting spatial interpolation technique, *Computers & geosciences*, 34, 1044–
- 370 1055, <https://doi.org/https://doi.org/10.1016/j.cageo.2007.07.010>, 2008.
- Marzorati, S. and Bindi, D.: Ambient noise levels in north central Italy, *Geochemistry, Geophysics, Geosystems*, 7, <https://doi.org/https://doi.org/10.1029/2006GC001256>, 2006.
- McNamara, D. E. and Buland, R. P.: Ambient Noise Levels in the Continental United States, *Bulletin of the Seismological Society of America*, 94, 1517–1527, <https://doi.org/10.1785/012003001>, 2004.
- 375 Mucciarelli, M., Gallipoli, M. R., Di Giacomo, D., Di Nota, F., and Nino, E.: The influence of wind on measurements of seismic noise, *Geophysical Journal International*, 161, 303–308, 2005.
- Peterson, J. R.: Observations and modeling of seismic background noise, Tech. rep., US Geological Survey, 1993.
- Presidency of Council of Ministers - Civil Protection Department : Italian Strong Motion Network, <https://doi.org/10.7914/SN/IT>, 1972.
- Ringler, A. and Hutt, C.: Self-noise models of seismic instruments, *Seismological research letters*, 81, 972–983, 2010.
- 380 Ringler, A. T., Evans, J. R., and Hutt, C. R.: Self-noise models of five commercial strong-motion accelerometers, *Seismological Research Letters*, 86, 1143–1147, 2015.
- Ringler, A. T., Steim, J., Wilson, D. C., Widmer-Schmidrig, R., and Anthony, R. E.: Improvements in seismic resolution and current limitations in the Global Seismographic Network, *Geophysical Journal International*, 220, 508–521, 2020.
- Schimmel, M., Stutzmann, E., Lognonné, P., Compaire, N., Davis, P., Drilleau, M., Garcia, R., Kim, D., Knapmeyer-Endrun, B., Lekic, V.,
- 385 Margerin, L., Panning, M., Schmerr, N., Scholz, J. R., Spiga, A., Tauzin, B., and Banerdt, B.: Seismic Noise Autocorrelations on Mars, *Earth and Space Science*, 8, e2021EA001 755, <https://doi.org/https://doi.org/10.1029/2021EA001755>, e2021EA001755 2021EA001755, 2021.
- Shapiro, N. M., Campillo, M., Stehly, L., and Ritzwoller, M. H.: High-resolution surface-wave tomography from ambient seismic noise, *Science*, 307, 1615–1618, 2005.
- 390 Stutzmann, E., Roult, G., and Astiz, L.: GEOSCOPE Station Noise Levels, *Bulletin of the Seismological Society of America*, 90, 690–701, <https://doi.org/10.1785/0119990025>, 2000.
- University of Trieste: Friuli Venezia Giulia Accelerometric Network, <https://doi.org/10.7914/SN/RF>, 1993.
- Vassallo, M., De Matteis, R., Bobbio, A., Di Giulio, G., Adinolfi, G. M., Cantore, L., Cogliano, R., Fodarella, A., Maresca, R., Pucillo, S., et al.: Seismic noise cross-correlation in the urban area of Benevento city (Southern Italy), *Geophysical Journal International*, 217,
- 395 1524–1542, 2019.

- Webb, S. C.: Broadband seismology and noise under the ocean, *Reviews of Geophysics*, 36, 105–142, 1998.
- Weber, E., Convertito, V., Iannaccone, G., Zollo, A., Bobbio, A., Cantore, L., Corciulo, M., Crosta, M. D., Elia, L., Martino, C., Romeo, A., and Satriano, C.: An advanced seismic network in the Southern Apennines Italy for seismicity investigations and experimentation with earthquake early warning, *Seismological Research Letters*, 78, 622–634, 2007.
- 400 Welch, P.: The use of fast Fourier transform for the estimation of power spectra: a method based on time averaging over short, modified periodograms, *IEEE Transactions on audio and electroacoustics*, 15, 70–73, 1967.
- Zambonelli, E., de Nardis, R., Filippi, L., Nicoletti, M., and Dolce, M.: Performance of the Italian strong motion network during the 2009, L’Aquila seismic sequence (central Italy), *Bulletin of Earthquake Engineering*, 9, 39–65, <https://doi.org/10.1007/s10518-010-9218-2>, 2011.

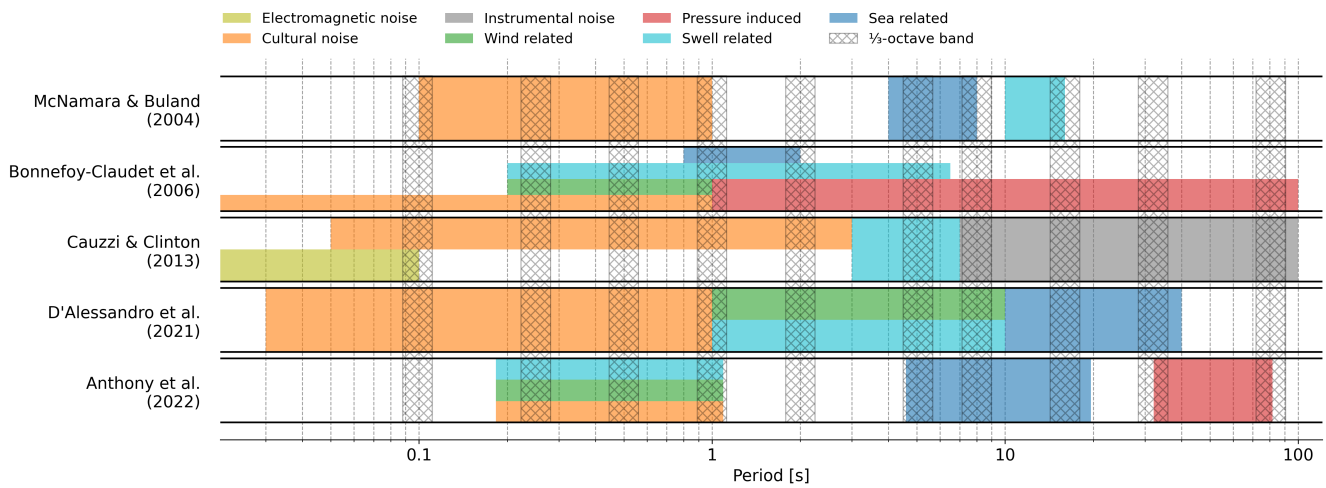


Figure 1. Main noise sources at different periods from the studies of McNamara and Buland (2004); Bonnefoy-Claudet et al. (2006); Cauzzi and Clinton (2013); D'Alessandro et al. (2021); Anthony et al. (2022). The hatched bands represent the one-third-octave bands used for the analysis.

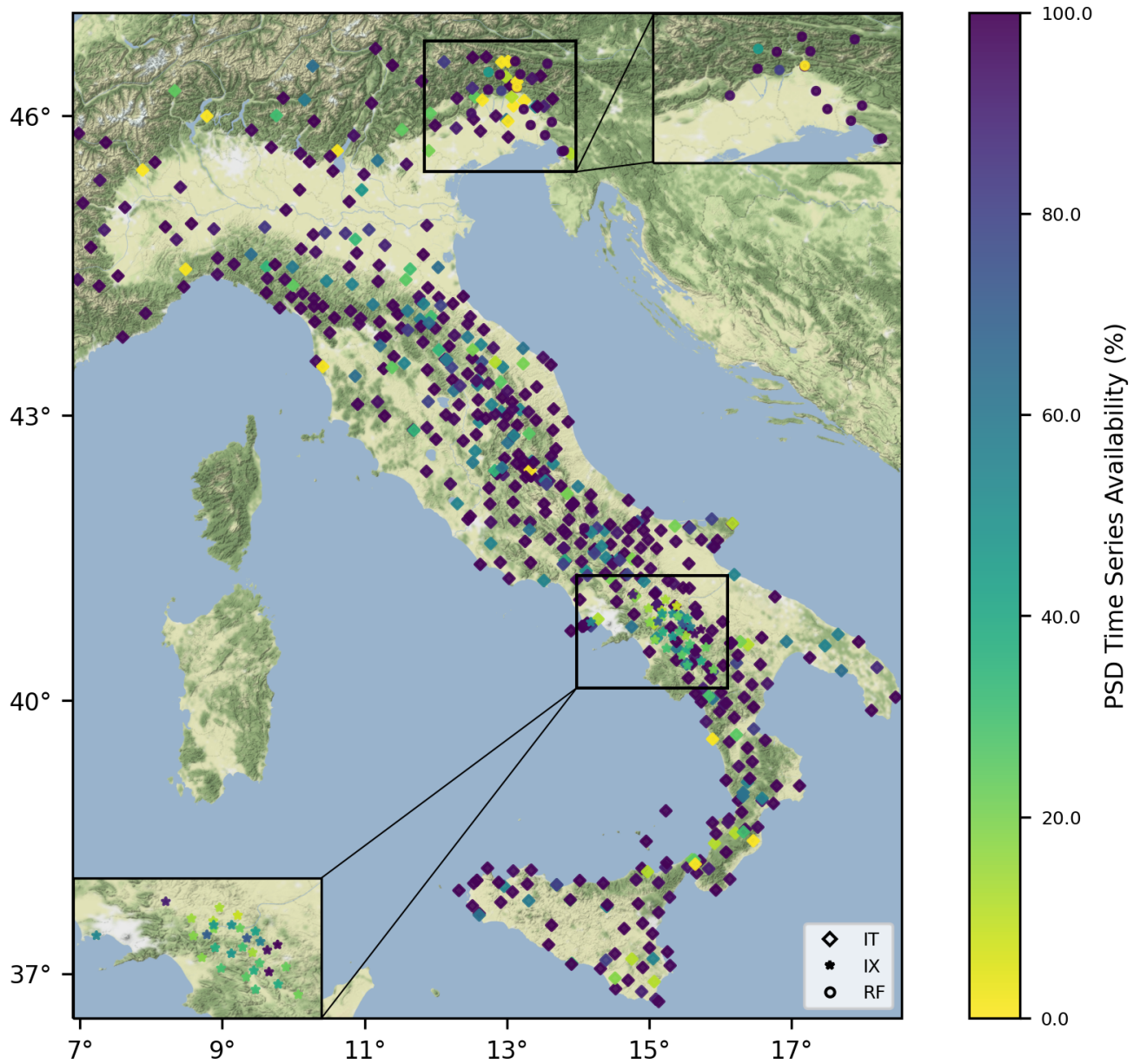


Figure 2. PSD time series availability of the RAN in 2022. The close-up boxes in the lower left and upper right highlight ISNet (IX) and RAF (RF), respectively. Basemap data are retrieved from © Stamen Design.

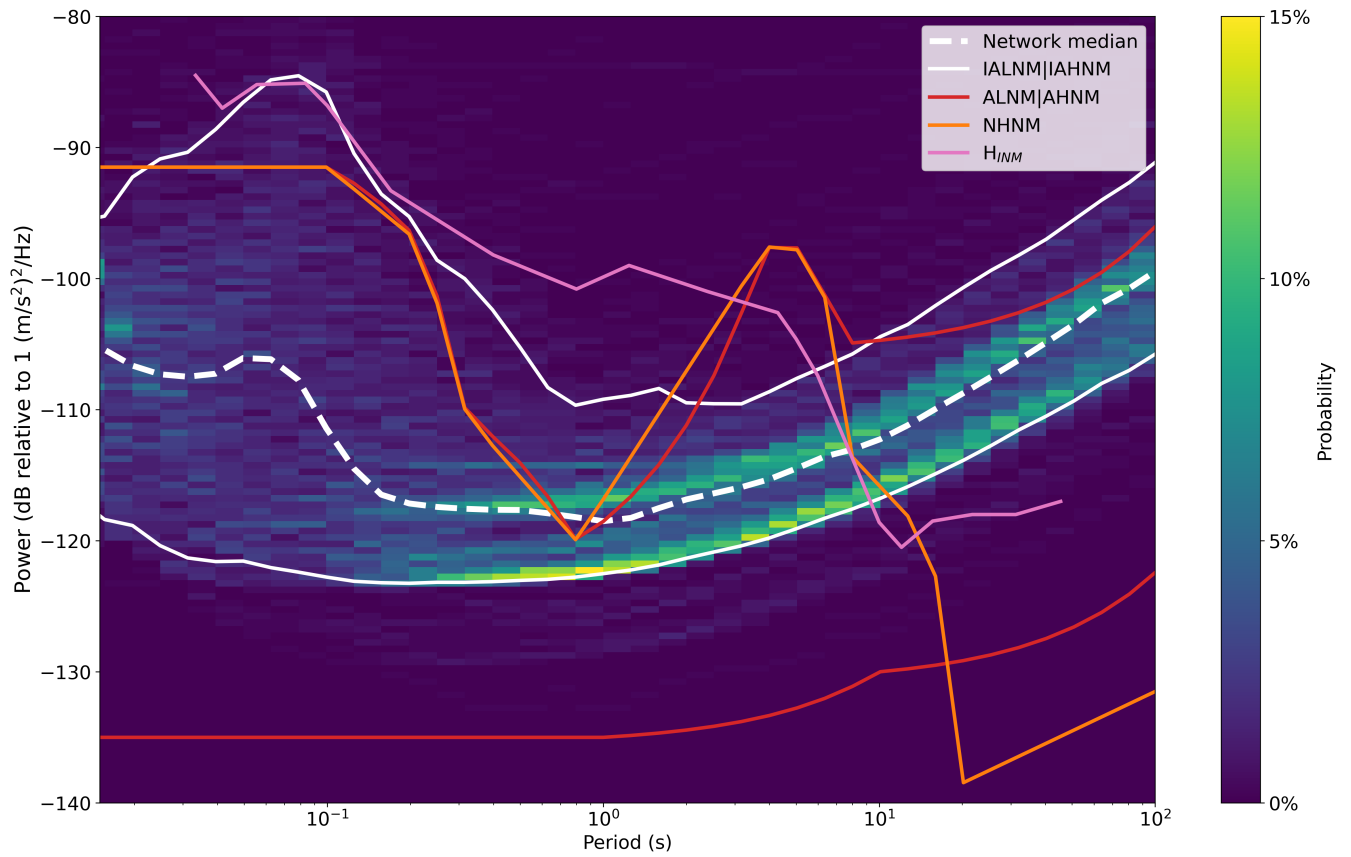


Figure 3. PSD probability density function of RAN. Dashed white line represents the median of the network and dotted lines are the 5% and 95% limits of the network. Solid green lines represent the ALNM and AHNM defined by Cauzzi and Clinton (2013). Red, and purple lines are NHNM and H_{INM} defined by Peterson (1993) and D’Alessandro et al. (2021), respectively.

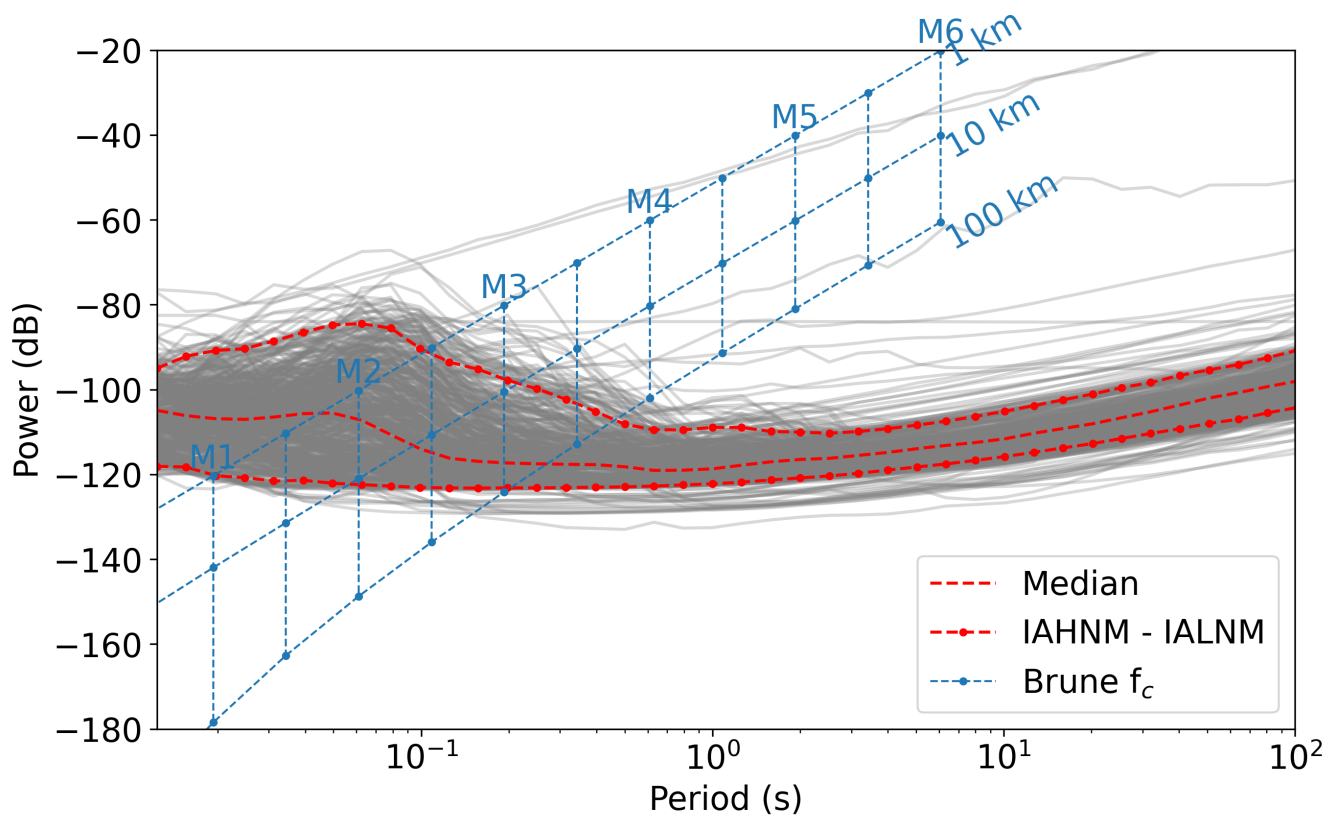


Figure 4. Median PSD of RAN stations (grey lines). Red dashed line and dots represent the median and IAHNM&IALNM, respectively.

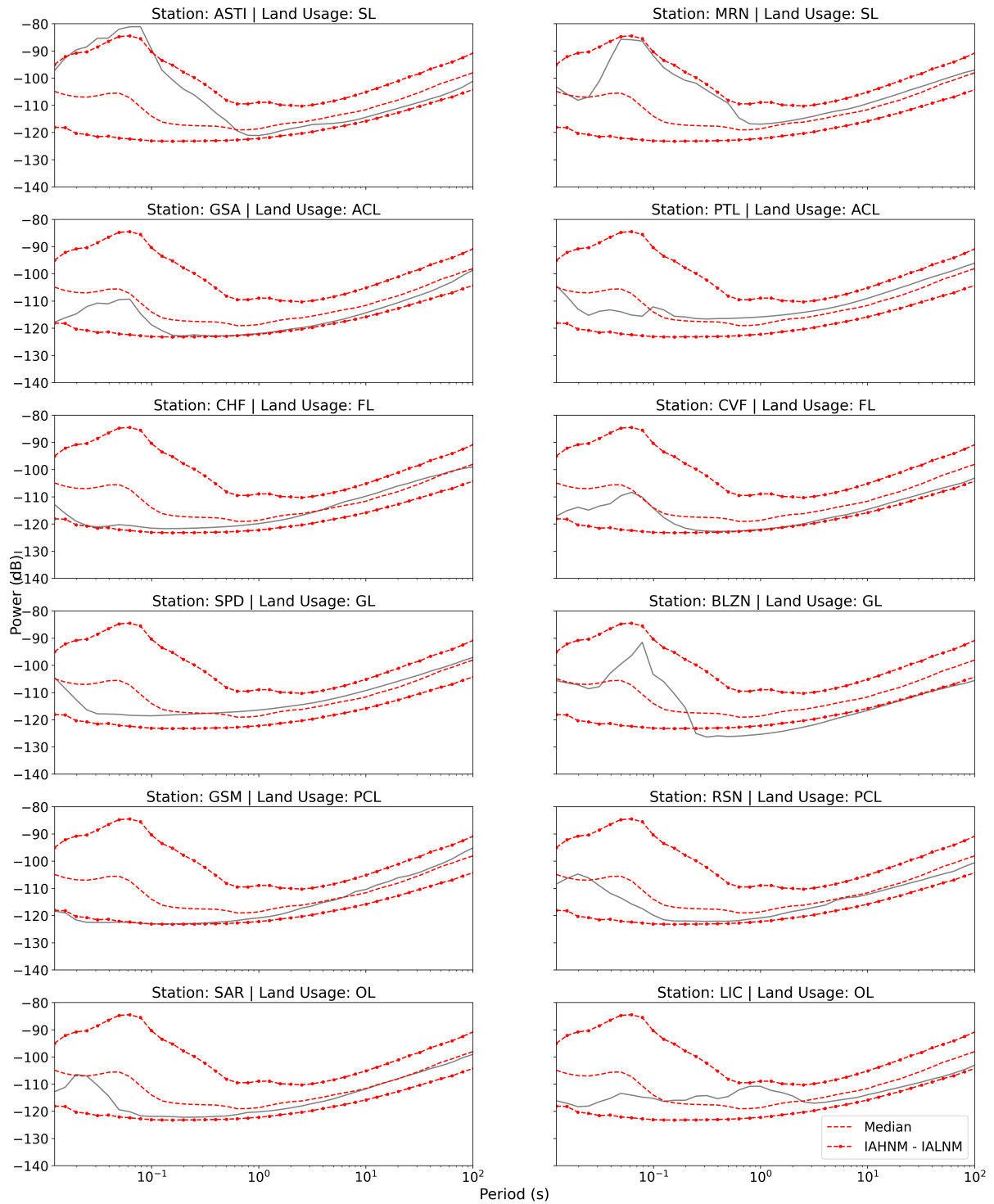


Figure 5. Median PSD of 2 randomly selected stations from each land usage type defined in Table 1. Red dashed line and dots represent the median and IAHNM&IAHNM, respectively.

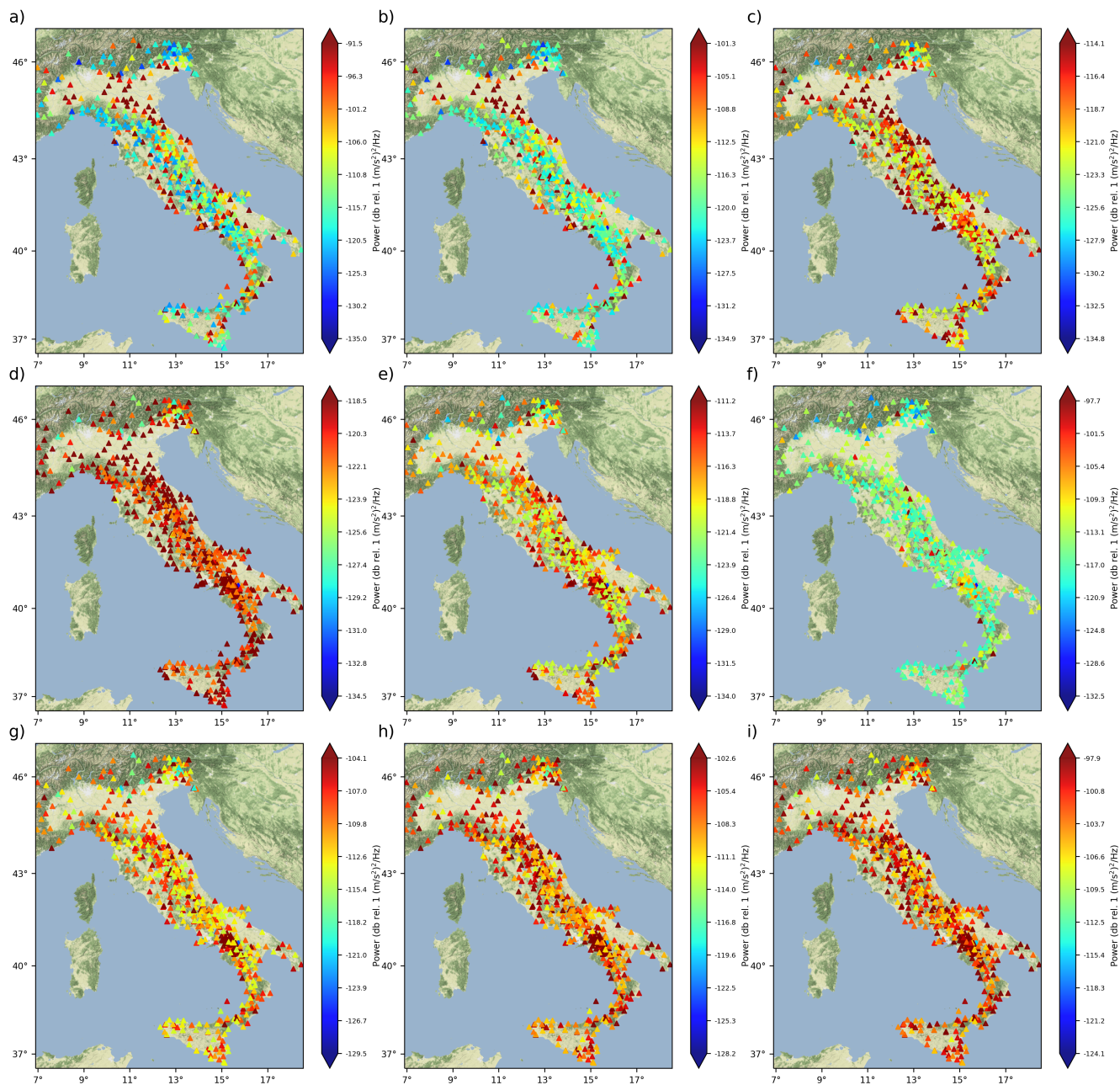


Figure 6. Median vertical component noise maps in one-third octave bands around a-i) 0.1 s, 0.25 s, 0.5 s, 1 s, 2 s, 5 s, 16 s, 32 s, and 80.6 s. Upper and lower limits of the color bar are defined by the model developed by Cauzzi and Clinton (2013). Background noise levels of all calculated periods can be found in Figure S1. Basemap data are retrieved from © Stamen Design.

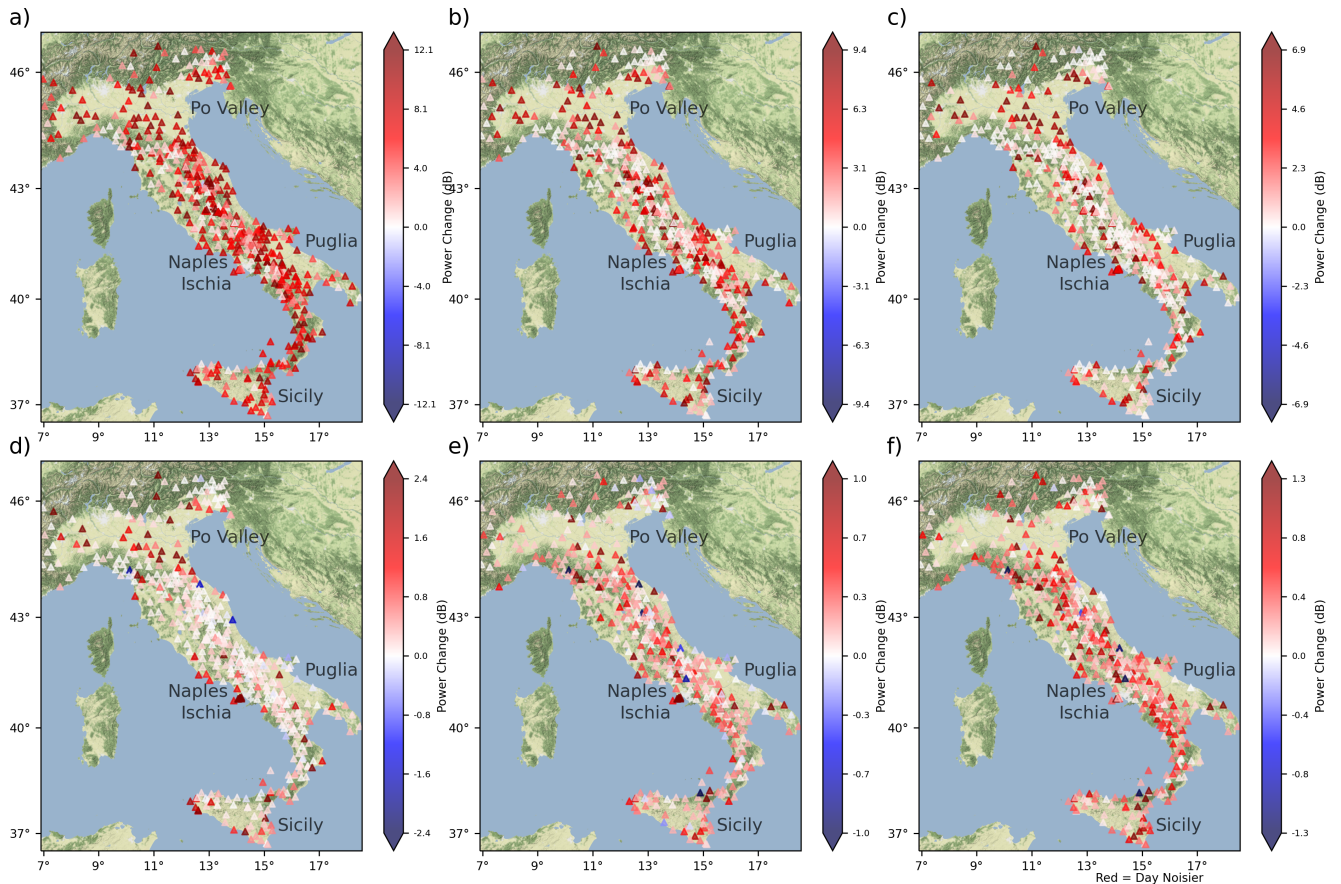


Figure 7. Difference between daytime and nighttime for the periods of a) 0.1 s, b) 0.25 s, c) 0.5 s, d) 1.0 s, e) 2.0 s, and f) 5.0 s in dB. Red color means day is noisier than night. Basemap data are retrieved from © Stamen Design.

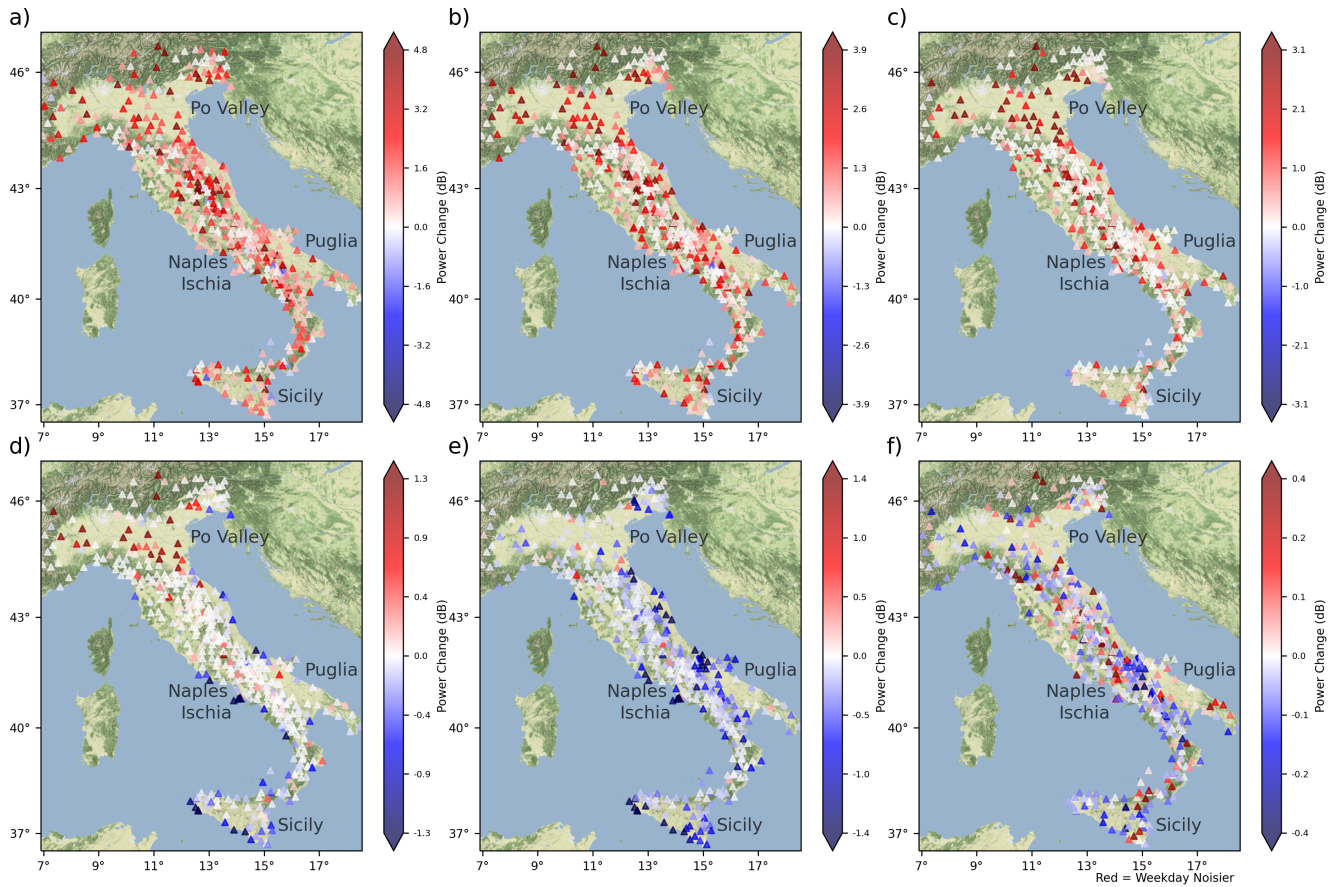


Figure 8. Difference between weekday and weekend time for the periods of a) 0.1 s, b) 0.25 s, c) 0.5 s, d) 1.0 s, e) 2.0 s, and f) 5.0 s in dB. Red color means weekday is noisier than weekend. Basemap data are retrieved from © Stamen Design.

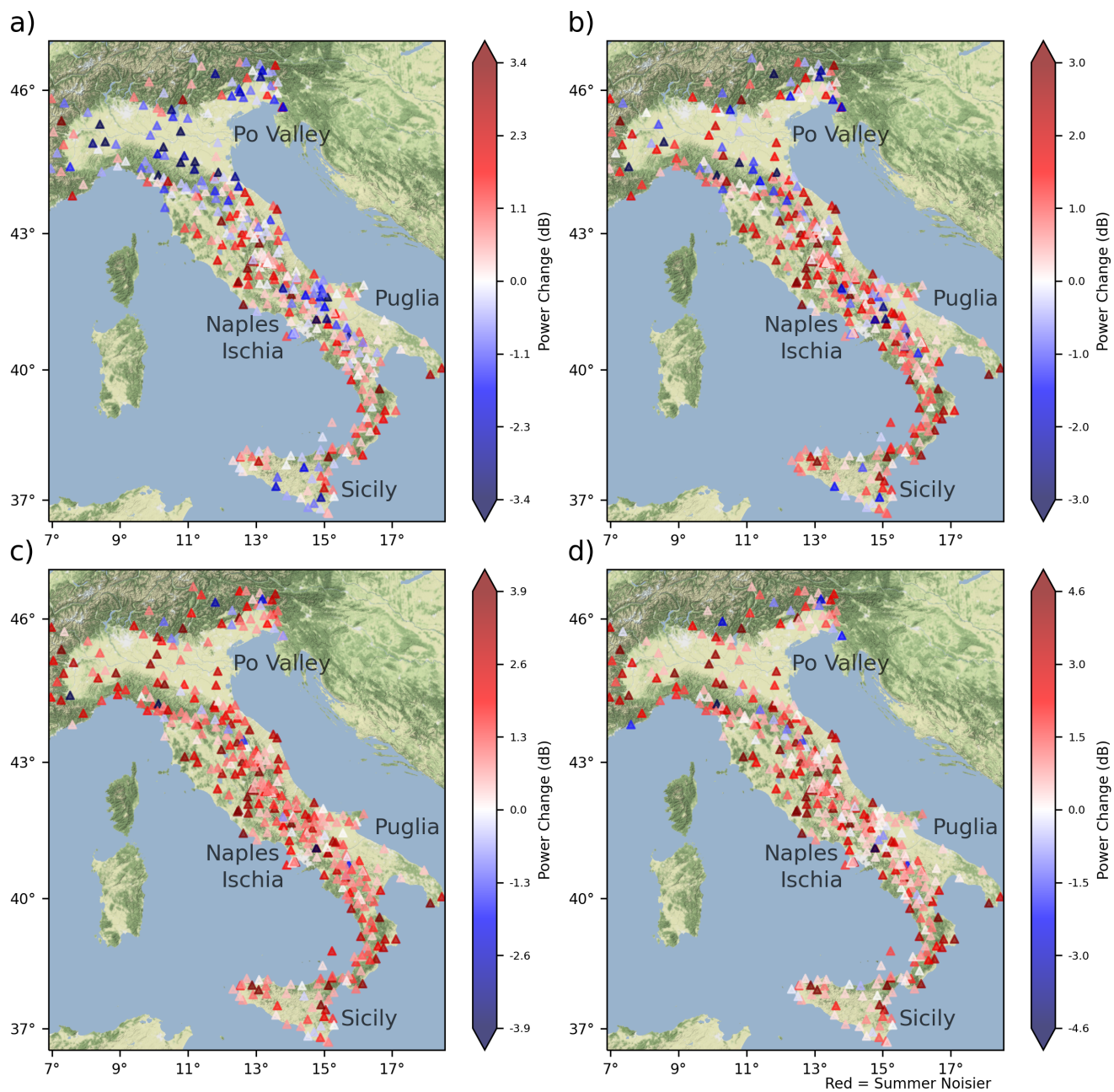


Figure 9. Seasonal median noise level change in dB for a) 5 s, b) 8 s, c) 16 s, and d) 32 s. Red color means summer is noisier than winter.



Figure 10. Geological Map of Trieste (grey, orange, and yellow colors indicate anthropic, ubiquitous deposit units, and flysch of Trieste, respectively), modified from Cucchi et al. (2013). Map on the lower right is created by using © Google Earth with satellite information from Landsat/Copernicus.

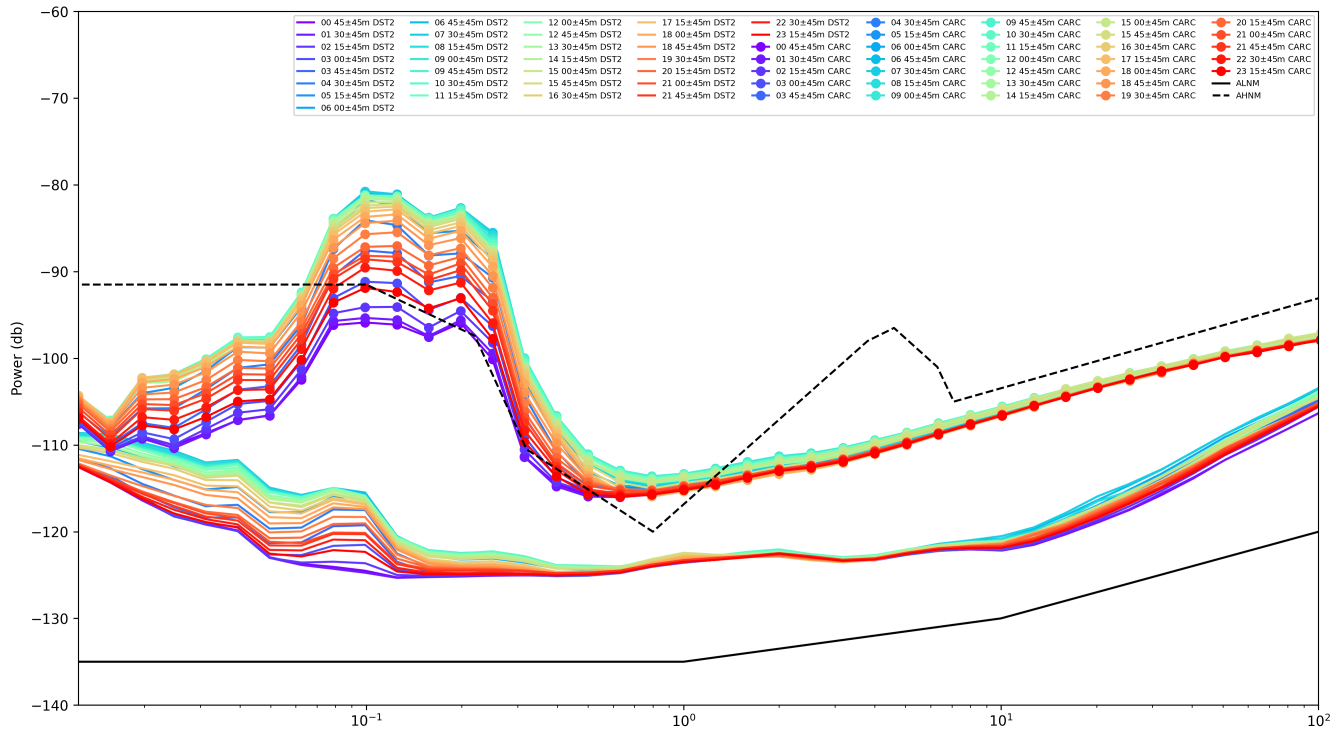


Figure 11. Hourly average plots of noise levels of DST2 (line) and CARC (line with dots). ALNM and AHNM introduced by Cauzzi and Clinton (2013) are black line and dashed line, respectively.

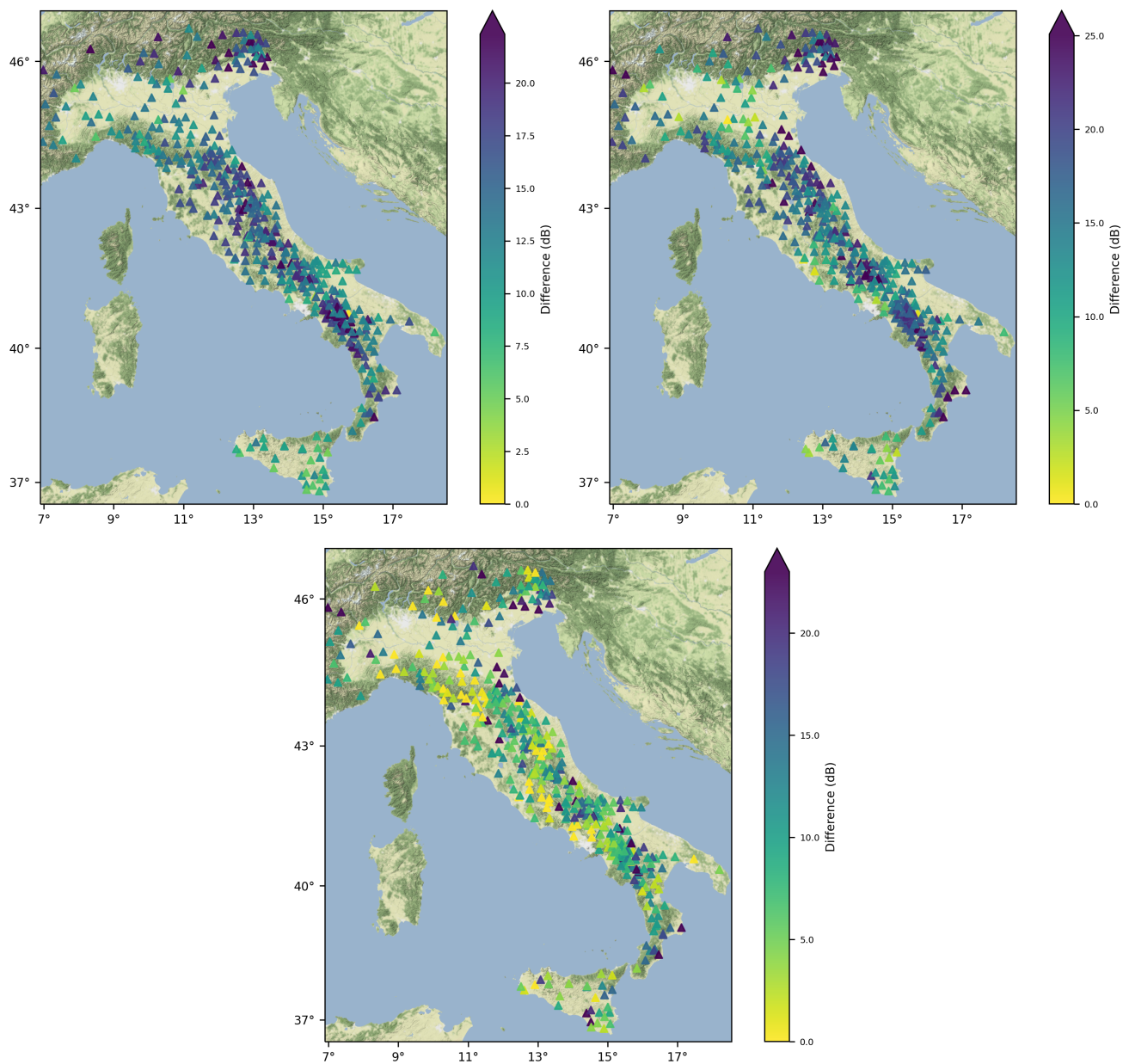


Figure 12. Difference between upper left) Band II, upper right) Band III, and bottom) Band IV of D'Alessandro et al. (2021) and our station. Band I is provided in Figure S7.

Table 1. Land usage at RAN stations (Istituto Superiore per la Protezione e la Ricerca Ambientale, 2022).

Land Usage	Code	Stations
Settlements	SL	424
Annual Cropland	ACL	56
Forest	FL	43
Grassland	GL	41
Permanent Cropland	PCL	14
Other land	OL	7

Table 2. Sensors at integrated RAN stations.

Sensors ^a	# Stations ^b	Sampling rate [Hz]
Kinematics EpiSensor	355	200
Syscom ms2007	180	200
Guralp CMG-5T	28	100
Reftek 147A	18	200
CFX US4H	3	200
Lunitek FB	1	250

^a Equipped with 24bit recorders

^b Status at 1st January 2022

Table 3. Soil conditions of integrated RAN stations (Felicetta et al., 2023).

EC8	# Stations
A	112
B	297
C	140
D	15
E	9
Unknown	12

Table 4. Data processing parameters for the evaluation of the PSDs of our study along with the studies of McNamara and Buland (2004), D’Alessandro et al. (2021), and Anthony et al. (2022).

Parameter	McNamara and Buland (2004)	Anthony et al. (2022)	Present work
	D’Alessandro et al. (2021)		
Window	60min	60min	90min
Window overlap	50%	50%	50%
Completeness	-	>90%	>90%
Sub-window	900s	819.2s	900s
Sub-window overlap	75%	75%	75%
Detrend	Linear	Linear	Linear
Gaps	Removed	Zero-pad	Linear interpolation
Window type	10% cosine	Hann	Hann
Binning/smoothing	Yes	None	None
Average	Overlapped 1 octave	1/3 octave	1/3 octave

Table 5. Number of stations in the network with median noise level exceeding AHNM for different periods.

Period (s)	AHNM Threshold	Exceeding stations	Percentage of network (%)	Land Usage					
				SL	ACL	FL	GL	PCL	OL
0.10	-91.50	57	11.54	49	5	1	0	1	0
0.25	-101.34	41	8.30	36	4	1	0	0	0
0.50	-114.06	92	18.62	81	7	1	1	1	1
1.00	-118.53	219	44.33	169	18	10	11	8	3
2.00	-111.20	34	6.88	27	1	1	4	0	1
5.04	-97.66	5	1.01	4	0	1	0	0	0
8.00	-104.91	15	3.04	10	1	1	2	0	1
16.00	-104.14	28	5.67	18	2	3	3	1	1
32.00	-102.60	57	11.54	42	0	3	5	1	2
64.00	-99.53	97	19.64	73	5	6	5	6	2
80.60	-97.93	79	16.00	59	4	6	5	3	2
Any	-	308	62.35	244	25	14	14	8	3